A nodal discontinuous Galerkin method with high-order absorbing boundary conditions and corner/edge compatibility

Axel Modave, Andreas Atle, Jesse Chan, Tim Warburton

A nodal discontinuous Galerkin method with high-order absorbing boundary conditions and corner/edge compatibility

Axel Modave[1,*], **Andreas Atle**[2], **Jesse Chan**[3], **Tim Warburton**[4]

[1]Team POEMS (CNRS-ENSTA-INRIA), Palaiseau, France
[2]TOTAL E&P, Houston, TX, USA
[3]Rice University, Houston, TX, USA
[4]Virginia Tech, Blacksburg, VA, USA

[*]Email: axel.modave@ensta-paristech.fr

Abstract

We present the coupling of a nodal discontinuous Galerkin (DG) scheme with high-order absorbing boundary conditions (HABCs) for the simulation of transient wave phenomena. The HABCs are prescribed on the faces of a cuboidal domain in order to simulate infinite space. To preserve accuracy at the corners and the edges of the domain, novel compatibility conditions are derived. The method is validated using 3D computational results.

Keywords: Transient waves, Discontinuous finite element, Absorbing boundary condition

1 Introduction

DG schemes are widely used for large-scale simulations of transient waves in complex media. For many applications, these schemes must be coupled with nonreflective boundary techniques in order to limit the size of the computational domain without losing accuracy or computational efficiency. In this context, PMLs and local HABCs are attractive since they provide high-fidelity solutions at reasonable computational cost. Nevertheless, HABCs have received far less attention than PMLs, and very few couplings with DG schemes have been proposed.

Local HABCs involve the computation of auxiliary fields governed by differential equations on the boundary (see *e.g.* [1, 2]), and require specific treatments at the corners of the domain. Hagstrom and Warburton [2] proposed compatibility conditions that preserve accuracy, but that are difficult to devise for complicated problems. In this work, we derive simpler compatibility conditions in the acoustic case by using a different representation for the HABCs.

2 HABC and compatibility conditions

Let the field $p(\mathbf{x},t)$ governed by the wave equation $\partial_{tt}p - \Delta p = 0$ in the cuboidal domain $\Omega = \{\mathbf{x}\in\mathbb{R}^3 : |x|<L_x, |y|<L_y, |z|<L_z\}$.

For each face, we consider HABCs derived using the $(2N+1)^{\text{th}}$ Padé approximation of the square root in the exact nonreflective condition [1]. On the face belonging to the plane $x = L_x$, we write the condition as

$$\partial_t p + \partial_x p = \frac{2}{M}\sum_{i=1}^{N} a_i \partial_t\big(p_i^x - p\big), \qquad (1)$$

where N auxiliary fields p_i^x are governed by

$$\partial_{tt}\left[b_i(p_i^x - p)\right] - \Delta_\perp^x p_i^x = 0, \quad \forall i\in[1,N], \quad (2)$$

with $a_i = \tan^2(i\pi/M)$, $b_i = a_i + 1$, $\Delta_\perp^x = \Delta - \partial_{xx}$ and $M = 2N+1$. This HABC is nearly identical to the one proposed by Collino [1]. It is equivalent to a special case of the one considered in [2], but the specific structure of Eqs. 1-2 leads to simpler compatibility conditions.

Additional relations must be defined on the border of each face (*i.e.* on the edges) because of the operator $\Delta_\perp^x$ in Eq. 2. Following [2], they are devised to ensure the compatibility of the system. On the edge belonging to the line $(x,y) = (L_x, L_y)$, the fields p_i^x and p_j^y defined on the adjacent faces then verify the boundary conditions

$$\partial_t p_i^x + \partial_y p_i^x = \frac{2}{M}\sum_{j=1}^{N} a_j \partial_t\big(p_{ij}^{xy} - p_i^x\big), \quad \forall i,$$

$$\partial_t p_j^y + \partial_x p_j^y = \frac{2}{M}\sum_{i=1}^{N} a_i \partial_t\big(p_{ij}^{xy} - p_j^y\big), \quad \forall j,$$

where N^2 auxiliary fields p_{ij}^{xy} are governed by

$$\partial_{tt}\Big[(1+a_i+a_j)p_{ij}^{xy} - b_i p_j^y - b_j p_i^x\Big] - \partial_{zz}p_{ij}^{xy} = 0, \quad \forall i,j. \quad (3)$$

Similarly, relations close to Eq. 2 are prescribed on the corners to give boundary conditions for the auxiliary fields defined on the edges. They involve N^3 auxiliary fields that are governed by algebraic relations on the corners.

3 Scheme and computational procedure

The scheme is written for the pressure-velocity system and based on the variational form

$$\begin{cases} \big((\partial_t p + \nabla\cdot\mathbf{u}),\phi\big)_{\Omega_k} = \big\langle \mathbf{n}\cdot(\mathbf{u}^{\text{in}}-\mathbf{u}^\star),\phi\big\rangle_{\Gamma_k} \\ \big((\partial_t \mathbf{u} + \nabla p),\boldsymbol{\psi}\big)_{\Omega_k} = \big\langle \mathbf{n}(p^{\text{in}}-p^\star),\boldsymbol{\psi}\big\rangle_{\Gamma_k} \end{cases} \quad (4)$$

with test functions ϕ and $\boldsymbol{\psi}$, a mesh cell Ω_k, its boundary Γ_k, and the external unit normal $\mathbf{n}$. Upwind fluxes are defined by taking

$$p^\star = (r^+)^{\text{in}} + (r^-)^{\text{ex}} \quad (5)$$

$$\mathbf{n}\cdot\mathbf{u}^\star = (r^+)^{\text{in}} - (r^-)^{\text{ex}} \quad (6)$$

where $r^\pm = p \pm \mathbf{n}\cdot\mathbf{u}$ are the outgoing $(+)$ and incoming $(-)$ characteristics. The subscripts $^{\text{in}}$ and $^{\text{ex}}$ denote interior and exterior values on Γ_k.

The HABC is incorporated in the scheme by rewriting Eq. 1 with characteristics. On the face belonging to the plane $x = L_x$, one has

$$r^- \overset{\text{(def.)}}{=} p - \mathbf{e}_x\cdot\mathbf{u} \overset{\text{(Eq. 1)}}{=} \frac{2}{M}\sum_{i=1}^{N} a_i(p_i^x - p).$$

This incoming characteristic is used in the upwind fluxes (Eqs. 5-6) on the domain boundary. Since the auxiliary fields are governed by 2D and 1D wave-like equations (Eqs. 2-3) on the faces and the edges, we use 2D and 1D versions of the variational form (Eq. 4). HABCs are prescribed on the auxiliary fields by using the same strategy. The procedure then consists in 3D/2D/1D solvers on the domain/faces/edges. For each mesh node of the edges and for each corner, the incoming characteristics are computed by solving systems with $2N$ and $3N^2$ unknowns. See [3] for the detailed procedure and GPU computational performance results.

4 Numerical results

We consider the propagation of a spherical wave in the cuboidal domain $\Omega = [-0.5, 0.5]^3$. The wave is generated using a point source at the position $(0, 0.1, 0.2)$ with a Ricker wavelet. We use a mesh composed of 70,895 tetrahedra, third-degree basis functions and a fourth-order Runge-Kutta scheme. Simulations are performed with HABCs of different orders. For each case, Figure 1 shows the time-evolution of the error

$$\sqrt{\frac{\|p-p_{\text{ref}}\|^2_{L_2(\Omega)} + \|\mathbf{u}-\mathbf{u}_{\text{ref}}\|^2_{L_2(\Omega)}}{\sup_{t>0}\left(\|p_{\text{ref}}\|^2_{L_2(\Omega)} + \|\mathbf{u}_{\text{ref}}\|^2_{L_2(\Omega)}\right)}},$$

where p_{ref} and $\mathbf{u}_{\text{ref}}$ correspond to the solution of the free-space problem defined on $\mathbb{R}^3$.

At the beginning, the error is dominated by the numerical error (the same in all the cases) generated when the wavefront is travelling inside Ω and has not reached the boundary yet. Later, a modeling error is generated because of the spurious reflection of waves at the boundary. The higher the order of the HABC, the smaller the error, which validates the method for short times. For long times, the error converges towards the same value for all the orders, except for $N = 0$ where the error remains decreasing. This is due to the poor long-time behaviour of Padé-type HABCs, which has been observed in 2D in [2]. We plan to extend the method for long-time simulations and other physical waves.

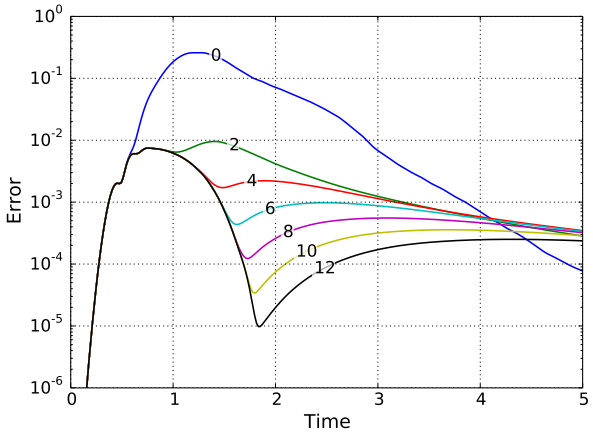

Figure 1: Error with HABCs having N additional fields ($N = 0, 2, \ldots, 12$). The main spherical wavefront is travelling in Ω when $t \in [0, 2]$.

This work was funded by a grant from TOTAL E&P Research and Technology USA.

References

[1] F. Collino (1993). "High-order absorbing boundary conditions for wave propagation models. Straight line boundary and corner cases". *Proceedings of WAVES 1993.*

[2] T. Hagstrom and T. Warburton (2004). "A new auxiliary variable formulation of high-order local radiation boundary conditions: corner compatibility conditions and extensions to first-order systems". *Wave motion* **39**(4), 327-338.

[3] A. Modave, A. Atle, J. Chan and T. Warburton (2016). "A GPU-accelerated nodal discontinuous Galerkin method with high-order absorbing boundary conditions and corner/edge compatibility". Preprint arXiv/abs/1610.05023.